

## Phonon dispersion in polycrystalline ice: Implications for the collective behavior of liquid water

A. Criado

*Instituto de Ciencia de Materiales, Departamento Física de la Materia Condensada, Universidad de Sevilla,  
P.O.Box 1065, E-41080 Sevilla, Spain*

F. J. Bermejo and M. García-Hernández

*Instituto de Estructura de la Materia, Consejo Superior de Investigaciones Científicas, Serrano 123, E-28006 Madrid, Spain*

J. L. Martínez

*Instituto de Ciencia de Materiales de Madrid, Universidad de Autónoma de Madrid, Facultad de Ciencias C-IV,  
E-28049 Cantoblanco, Madrid, Spain*

(Received 17 August 1992)

The steep phonon-dispersion curves found in computer-simulation studies on normal and super-cooled water which have been interpreted as evidence of the existence of "fast-sound modes" of kinetic origin are considered. From the analysis of the dynamical structure factor of polycrystalline ice it is shown that such features are present in the solid calculated within the harmonic approximation, and the anomalous steep increase in frequency is shown to be originated by optical phonon branches, which cross the acoustical ones at wave vectors below the zone center, and result in a pull-out up to a maximum frequency at  $Q_p/2$ , which roughly coincides with that of the sharp translational edge.

PACS number(s): 61.20.-p, 64.70.-p

### I. INTRODUCTION

The existence of propagating collective modes in liquid binary mixtures composed by particles with disparate mass ratios, which are additional to those of a normal sonic origin, has been predicted from calculations based upon kinetic theory [1] and computer simulations [2]. However, the experimental verification of such a prediction is constrained mostly to the hydrodynamic region where some evidence has been adduced on the basis of light-scattering studies [3], although some claims of observation of a similar phenomenon on binary mixtures of dense gases have also been reported [4].

Liquid water was also expected to show such a behavior due to the different masses of its constituent atoms [2]. From computer-simulation studies [5-7] as well as from calculations based on the Mori formalism using a reduced dynamical variable which does not take explicitly into account the intramolecular bonding [7], the existence of such high-frequency features was inferred. Even further, experimental evidence for the presence of such an excitation was also adduced from a rough analysis of coherent inelastic-neutron-scattering (INS) spectra from liquid water [8].

From previous experience with the analysis of inelastic-neutron-scattering spectra as well as molecular-dynamics (MD) simulations of a related material (methanol) in its liquid [9], glass, and crystalline modifications [10], it became clear that, because of the presence of lower-lying optical branches in the crystalline solid, an apparently anomalous steep frequency versus wave vector curve

could result from the orientational (polycrystalline) averaging of the single-crystal spectra. That such a feature characteristic of the polycrystalline solid was also present in the cold liquid was evidenced from comparison of experimental INS results with MD calculations for the liquid and lattice-dynamics (LD) results for the polycrystalline solid [9]. As a consequence, an apparently acoustical branch appears in the liquid phase when the frequencies corresponding to the maxima of the  $S(Q, \omega)$  dynamic structure factors (or the longitudinal current-current autocorrelation function) are plotted against the wave vector. Such a plot then shows frequencies far exceeding those which are a prolongation of hydrodynamic sound, and therefore, only after a detailed analysis can the physical origin of such a feature be clarified.

The aim of the present paper is, therefore, to help to clarify the origin of what is observed in the computer simulations of liquid water by means of the analysis of the dispersion behavior of polycrystalline ice. The rationale of such an approach lies in the noticeable similarity of the features observed in cold liquids and polycrystals at the length and time scales accessible to neutron spectroscopy and computer simulations, once the differences in elastic constants and phonon lifetime effects are taken into account. As a matter of fact, the remarkable similarities between the short-range structure of the cold liquid and the solid, and the fact that the extent of real space explored by INS or simulation techniques becomes comparable with the correlation length of the liquid phase, explain the origin of such similitude. For such a purpose a lattice-dynamical calculation was carried out following

the same lines adopted in previous work [9], thus aiming to help to rationalize the rather disparate interpretations of MD results currently appearing in the literature.

## II. COMPUTATIONAL DETAILS

For the pressures and temperatures of our interest the relevant form of ice is hexagonal (Ih), which shows four molecules in the unit cell [11] where each oxygen atom is surrounded by four other oxygen atoms with tetrahedral coordination. The hydrogen atoms are disordered with an occupancy factor of 0.5 and lie on the lines joining the oxygens, with one hydrogen atom on every line. Because of its disordered structure, it is difficult to settle a lattice-dynamical model for hexagonal ice. There have been a large number of attempts in the literature to work out a model able to reproduce the  $Z(E)$  experimental density of vibrational states (DOS) with varying degrees of sophistication. The first ones treated the molecules as point masses [12] in order to model the translational modes. Because of the fact that both hexagonal and cubic modifications present tetrahedral coordination and that their Raman and infrared spectra are rather similar, a further model was proposed [13] using the cubic lattice and imposing order on the hydrogen atoms. A short-range force field was used and the calculated DOS showed a remarkable agreement with experiment, surely because of the similar crystal coordinations of both structures. We have tried this model using a more sophisticated force field composed of a short-range part plus a long-range one which accounts for the Coulombic interactions. Although the calculated frequency distributions (DOS) were found to be in acceptable agreement with experiment [14] some instabilities appeared for certain wave vectors. However, this model turned out to be useless for calculating the neutron-inelastic-scattering function  $S(Q, \omega)$  since it evidenced some important disagreements with the available data concerning the dispersion curves for the single-crystal [15] solid.

Fortunately, an ordered low-temperature, low-pressure ice structure has been recently found experimentally under special conditions [16], where the oxygen atoms lie on a lattice identical with that of hexagonal ice. This structure is orthorhombic and has been used successfully in this work to model the lattice dynamics and neutron scattering in hexagonal ice.

Other reported approaches use the fully disordered structure where the dynamical problem is addressed by means of computer molecular dynamics [17] or by brute-force diagonalization of the dynamical matrix [18, 19]. However, there is a widely accepted consensus that, unless one is particularly interested in the details concerning the high-frequency librational band (above 10 THz), the most relevant features regarding the motions below such frequency cutoff are reasonably well reproduced by the LD calculations performed on proton-ordered structures [20].

Several potential function models using Lennard-Jones functions for the short-range part and point charges for Coulombic interactions are available in the literature for water molecules [21, 19]. We have selected the SPC po-

tential [21], which has been shown to provide an excellent agreement with the measured elastic constants of ice Ih as well as predicts the correct pressure-induced transitions [20], and also, in order to explore the robustness of our predictions, we have checked that the results are very similar using some other ones [transferable interaction potential with four points (TIP4P), in particular]. As a first check, the minimum-energy crystal configuration was calculated by means of a Newton-Raphson procedure starting at the orthorhombic experimental structure. The maximum lattice-parameter relative change was only 4.6%, confirming the validity of the adopted potential model. The LD calculation was carried out using the optimal (energy minimized) crystal configuration by means of our own code [22].

The calculated DOS has been obtained by means of a fine sampling of  $40 \times 40 \times 40$  points in the Brillouin zone of the crystal and the resulting frequencies have been binned into a histogram. Figure 1(a) shows both

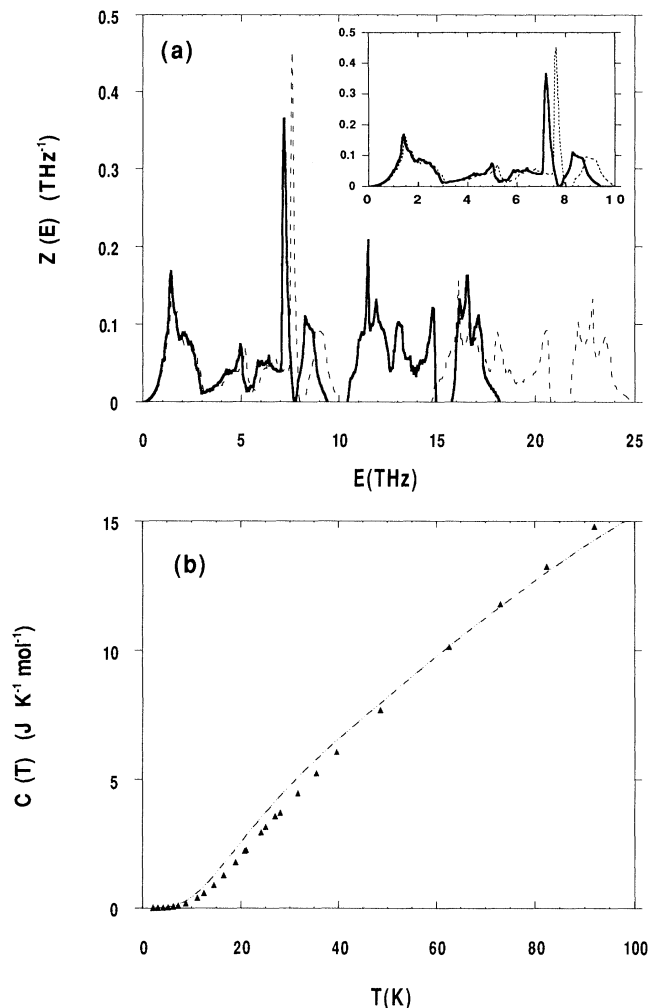


FIG. 1. (a) Calculated  $Z(E)$  densities of vibrational states (DOS) for  $\text{D}_2\text{O}$  ice (solid line) and  $\text{H}_2\text{O}$  ice (dashed line). The inset shows the translational region on an expanded scale. (b) A comparison between the experimentally measured heat capacity  $C(T)$  for  $\text{H}_2\text{O}$  ice (full triangles) and the calculated quantity which is shown as a dash-dotted curve.

frequency distributions as calculated for both light- and heavy-water ices, and an assessment of the reliability of the calculated distributions can be made from comparison of the specific heat curves corresponding to calorimetric measurements [23] with that computed using the resulting DOS for light-water ice, which are shown in Fig. 1(b) for the the range of temperatures where the anharmonic contribution is rather small [14]. As it can be seen from the figure the computed and measured curves for the  $C(T)$  heat capacity are in rather good agreement, being the maximum discrepancy located about 10 K. The origin of such a discrepancy is not understood at present, but it seems to be an ubiquitous feature in the comparison between calculated and calorimetric heat capacities reported so far [13].

The coherent inelastic-neutron-scattering intensities

$$F_1(\mathbf{Q}, \mathbf{q}_j) = \sum_k \sum_i b_i e^{-W_i} \mathbf{Q} \cdot [\mathbf{e}^t(\mathbf{q}, k_j) + \mathbf{e}^r(\mathbf{q}, k_j) \times \mathbf{x}(ki)] \times \exp[i\mathbf{Q} \cdot \mathbf{x}(ki)] \exp[i\mathbf{G} \cdot \mathbf{x}(k)], \quad (2)$$

where  $i$  labels the different atoms in the molecule  $k$ ,  $b_i$  is the coherent scattering length of atom  $i$ ,  $W_i$  is the Debye-Waller factor,  $\mathbf{x}(k)$  is the position vector of the center of mass of molecule  $k$  and  $\mathbf{x}(ki)$  is the position vector of atom  $i$  belonging to molecule  $k$  with respect to its center of mass, and  $\mathbf{e}^r(\mathbf{q}, k_j)$  and  $\mathbf{e}^t(\mathbf{q}, k_j)$  are the rotational and translational components of the polarization vectors. The calculation has been performed using thermal parameters compatible with those of ice Ih for  $T = 88$  K.

In order to allow a comparison with optical spectroscopic data [25], the limiting frequencies at  $Q \approx 0$  have been evaluated and a comparison between experimental results from INS [14] and Raman and infrared [25] is given in Table I for the set of 21 modes (the three acoustical lattice modes at  $Q = 0$  are disregarded). Taking into account the difficulties in extracting accurate frequency values from the broad features present in the experimental spectra [25], the agreement between the calculated and observed lattice frequencies can be considered to be quite reasonable.

For the polycrystal, the relevant scattering function  $S(Q, \omega)$  must be obtained as an average over all scattering directions  $\mathbf{Q}$  [26]. This process has been carried out by dividing the  $Q$  space in a fine mesh ( $40 \times 40 \times 40$  points in the first Brillouin zone). In order to provide a range of  $Q$  values compatible with both the MD simulation and the experiments, the explored extent in the reciprocal space was set to  $0.1 \text{ \AA}^{-1} \leq Q \leq 4.5 \text{ \AA}^{-1}$ . This implies that the range of interparticle distances in real space will be confined within the interval  $1.396 \text{ \AA} \leq r \leq 62.8 \text{ \AA}$ .

Because of the large number of phonon peaks appearing in  $S(Q, \omega)$  once the polycrystalline average is performed, it is obviously difficult to assign an average frequency to the observed excitations. In order to define such a quantity, we have evaluated the first even-

have been calculated within the one-phonon approximation, where the scattering at a dispersion vector  $\mathbf{Q}$  is governed by the momentum and energy conservation laws  $\mathbf{Q} = \mathbf{G} - \mathbf{q}$  and  $E - E_0 = \pm \hbar\omega(\mathbf{q})$ .  $E$  and  $E_0$  are the energies of the scattered and incident neutrons, respectively,  $\mathbf{G}$  is a reciprocal-lattice vector, and  $\omega(\mathbf{q})$  is the frequency of the phonon ( $\mathbf{q}_j$ ) involved in the process.

The dynamic structure factor corresponding to coherent one-phonon scattering processes  $S(\mathbf{Q}, \omega)$  can be written in the following way for molecular systems [24]:

$$S(\mathbf{Q}, \omega) \text{ (mode } \mathbf{q}_j) = \frac{\delta(E_j(\mathbf{q}) \pm \frac{1}{2} \hbar\omega_j(\mathbf{q}))}{\omega_j^2(\mathbf{q})} |F_1(\mathbf{Q}, \mathbf{q}_j)|^2 \quad (1)$$

with

frequency moments of the scattering law which are defined as

$$\mu_n = \int_{-\infty}^{\infty} d\omega \omega^n S(Q, \omega), \quad (3)$$

$$\omega_0^2 = \mu_2 / I(Q), \quad (4)$$

$$\omega_t^2 = \mu_4 / \mu_2, \quad (5)$$

$$I(Q) = \mu_0. \quad (6)$$

TABLE I. Calculated frequencies (in THz) at zero-momentum transfers for all the optical modes of light- and heavy-water ices.

Mode	D <sub>2</sub> O ice			H <sub>2</sub> O ice		
	LD	INS	IR Raman	LD	INS	IR Raman
1	0.96			1.01		
2	1.50	1.64	1.64	1.58	1.71	1.70
3	4.82	4.47	4.68	4.97	4.59	4.92
4	5.85		6.05	6.19		6.38
5	7.26	6.63	6.62	7.63	6.87	6.86
6	7.62			7.84		
7	7.66			7.94		
8	8.77	8.85	8.54	9.35	9.16	8.99
9	9.36			9.91		
10	10.57			14.88		
11	11.11			15.69		
12	11.31			15.76		
13	11.33			15.91		
14	12.42	12.57	12.74	17.46	16.95	16.64
15	13.14			18.07		
16	13.55			18.65		
17	14.52			20.47		
18	16.17			22.07		
19	16.40	16.32	16.64	22.73	22.03	23.08
20	16.98			23.34		
21	18.17	21.52	19.18	24.76	29.26	25.19

The rationale behind the use of moments lies in the fact that, as shown in recent works on the thermodynamics of highly anharmonic crystals [27], reasonable coarse-grained approximations for the spectral shape can be obtained from the knowledge of the first even-frequency moments, and, on the other hand, can be compared with thermal and mechanical quantities in the long-wavelength limit. The square root of the second frequency moment,  $\omega_0$ , has the meaning of a physical frequency with a hydrodynamic limit given by  $v_{\text{eff}}Q$ , where  $v_{\text{eff}}$  is the average sound velocity defined in terms of the longitudinal and transverse sound velocities [28] (i.e.,  $3/v_{\text{eff}}^3 = 1/v_l^3 + 2/v_t^3$ ). It should be noticed that the huge elastic intensity has been subtracted and therefore  $I(Q)$  plays the role of an inelastic structure factor and not of a static  $S(Q)$ .

On the other hand, and in order to compare with the published results for liquid water, the frequency position versus wave vector of the main peaks in the dynamic structure factor  $S(Q, \omega)$  or those corresponding to its  $J_l(Q, \omega) = \omega^2/Q^2 S(Q, \omega)$  longitudinal current counterpart have also been evaluated from spectra which were binned into larger frequency channels in order to remove their  $\delta$ -like character. The maxima of the spectral envelopes of  $J_l(Q, \omega)$  are denoted as  $\omega_{\text{max}}$ . The latter quantity is most commonly plotted in MD works on the liquid phase, and in this case at least two different spectral bands are clearly seen.

### III. RESULTS

From inspection of Fig. 1(a) it can be seen that the main effects related to the motion of the hydro-

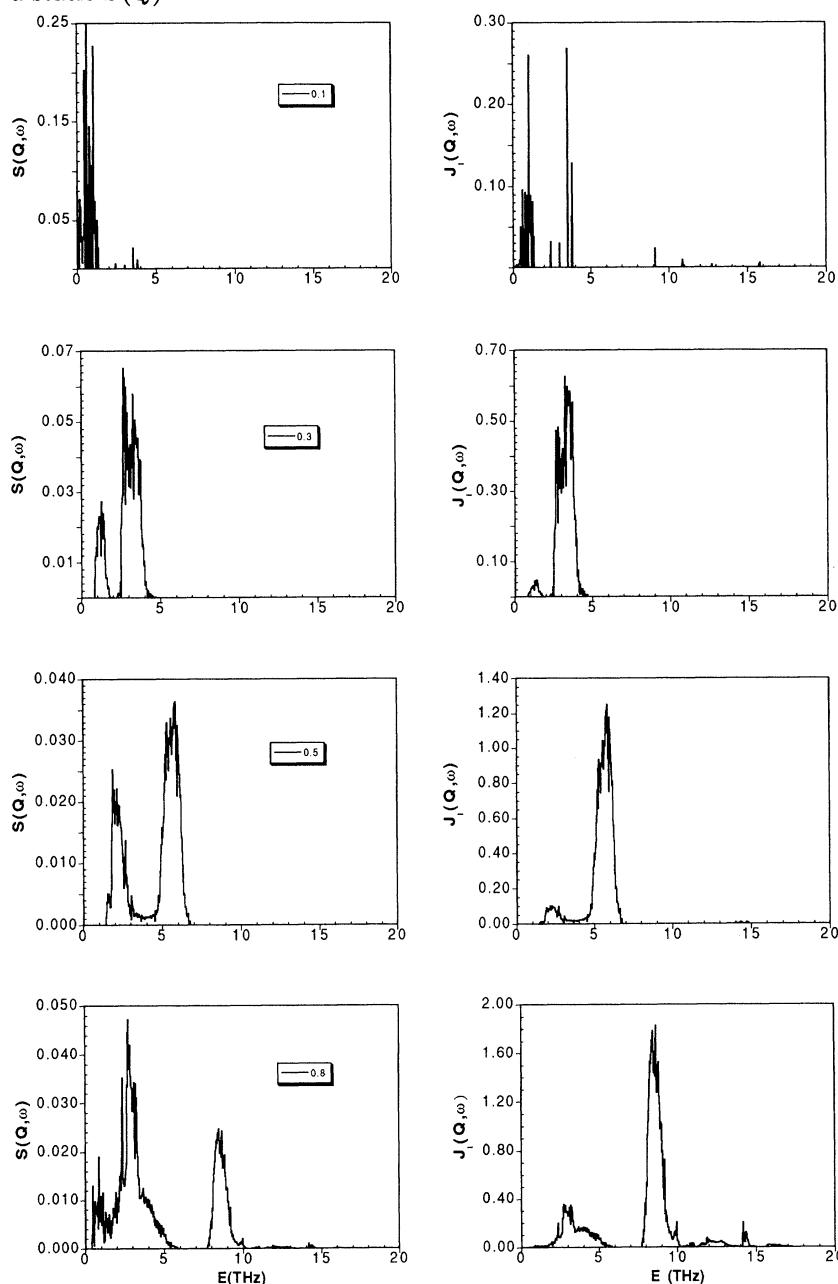


FIG. 2. Calculated  $S(Q, \omega)$  dynamic structure factors (left column) and the corresponding  $J_l(Q, \omega)$  longitudinal current correlation functions for a sample of the lowest wave vectors within the first Brillouin zone corresponding to polycrystalline  $D_2O$  ice. The momentum-transfer value for each graph is given within each frame in inverse angstrom units.

gen (deuterium) atoms are mainly confined to the high-frequency librational band, which, due to the large difference in atomic masses between hydrogen and deuterium, is shifted to higher frequencies in  $\text{H}_2\text{O}$  ice. Some values regarding the isotopic frequency shifts have been computed, and, for the translational band, the ratios of frequencies corresponding to the same peaks in light- and heavy-water ice are rather close to the square root of the ratio between the molecular masses. The shifts in this region are between 1.034 and 1.07, which compares very favorably with those derived from experimental measurements by Li *et al.* [14] which range between 1.03 and 1.05. The corresponding ratios for the librational band are within the interval 1.37–1.41 (close to the square root of the mass ratio of deuterium to hydrogen), which evidences the strong rotational character of these excitations, and are also in good agreement with experiment where values between 1.35 and 1.38 were found [14].

The analysis of the mode eigenvectors corresponding to the main peaks in the  $Z(E)$  was also performed. As expected, no clear separation between translational and rotational motions was found, even for the low-frequency (“translational”) band, since all the modes show a marked translation-rotation character, except in the  $Q = 0$  limit.

A set of  $S(Q, \omega)$  dynamic structure factors as well as the corresponding  $J_l(Q, \omega)$  functions for wave vectors spanning the first Brillouin zone is shown in Fig. 2. As it can be easily seen, purely acoustic manifolds are clearly visible in the  $S(Q, \omega)$  spectra as well as in the  $J_l(Q, \omega)$  correlations, although in this latter case most of the spectral power is transferred to the strong optical peak, ex-

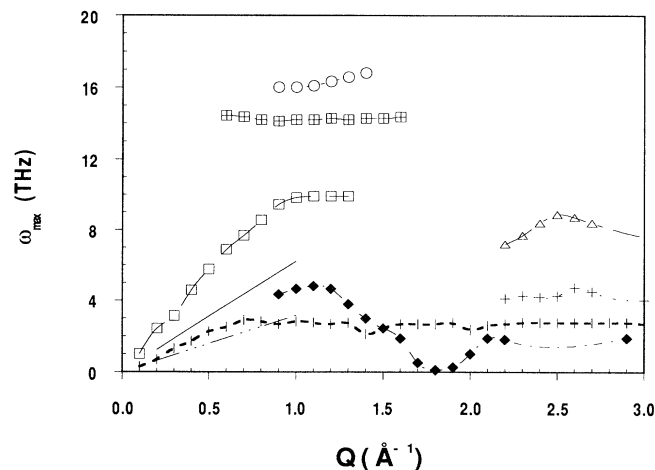


FIG. 3. The  $\omega_{\max}$  frequencies corresponding to the most prominent peak envelopes of  $J_l(Q, \omega)$  for excitations below 20 THz. The hydrodynamic dispersion for longitudinal sound is given as a straight solid line and that corresponding to transverse sound by a dash-dotted line. The open squares represent the apparent dispersion of the most intense peak. The line with vertical bars has been assigned a mostly transverse-sound character (see text), and the one with solid lozenges follows characteristics assignable to longitudinal sound. The open circles, open squares with crosses, crosses, and open triangles depict the apparent dispersion of peak envelopes of small intensity appearing in the calculated functions.

cept for the lowest explored wave vector ( $Q = 0.1 \text{ \AA}^{-1}$ ). As a matter of fact, from inspection of Table I as well as from the analysis of the dispersion branches [15] it can be seen that for wave vectors above  $0.1 \text{ \AA}^{-1}$  (about 0.28 in reduced units) the lowest-lying branches which correspond to those with frequencies at  $Q \approx 0$  of about 1.64 THz cross the three acoustical dispersion relations. At higher momentum transfers, most of the spectral power is dominated by the intense peak which is characterized by a strong frequency dependence and reaches a plateau value of about 10 THz at  $Q = 1 \text{ \AA}^{-1}$  and shows a van-

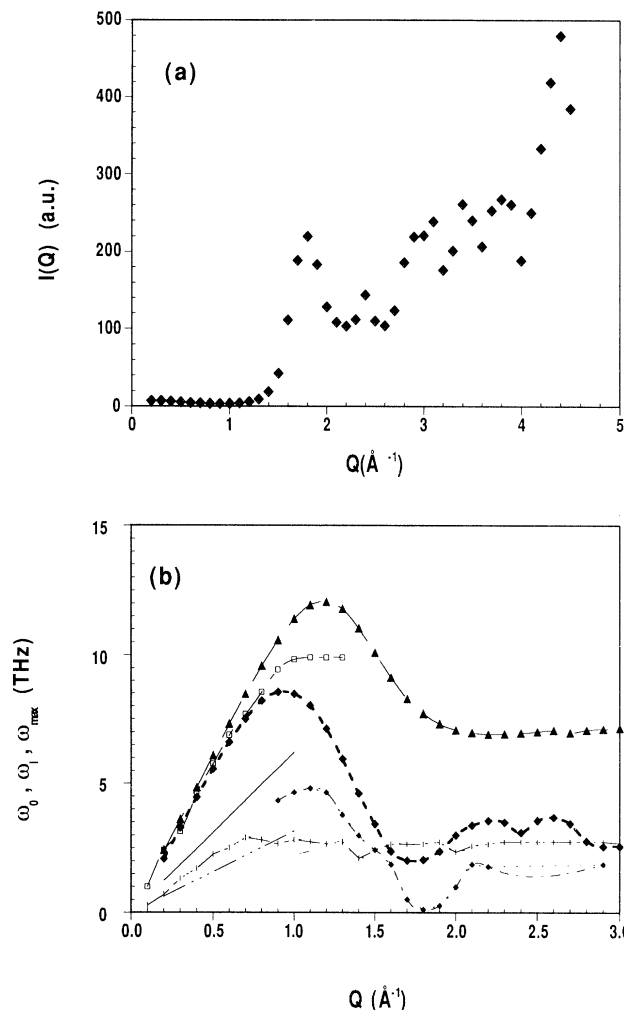


FIG. 4. The upper frame shows the  $I(Q)$  inelastic structure factor as calculated from Eqs. (3)–(6). The lower frame shows a comparison of the  $Q$  dependence of  $\omega_0, \omega_l$ , the square root of the  $\mu_0^2, \mu_l^2$  spectral moments with the  $\omega_{\max}$  peak frequencies (see text). The filled triangles and large filled lozenges show the  $Q$  dependence of  $\omega_l$  and  $\omega_0$ , respectively. Open squares give the dispersion of the most prominent peak in  $J_l(Q, \omega)$ . Small lozenges and vertical bars denote the  $\omega_{\max}$  frequencies of peak envelopes of mostly longitudinal- and transverse-sound origin. The solid and dash-dotted lines correspond to the dispersion of longitudinal and transverse hydrodynamic sound as measured by light scattering by Gagnon *et al.* [25].

ishing intensity for wave vectors higher than  $1.3 \text{ \AA}^{-1}$ .

The wave-vector dependence of  $\omega_{\max}$ , the frequency of the most relevant maxima in  $J_l(Q, \omega)$  is shown in Fig. 3. The most noticeable feature regarding this figure is the clear manifestation of the sound modes which are seen as small peaks in Fig. 2 at frequencies well below those of the most prominent band (up to 3 THz at  $Q = 0.8 \text{ \AA}^{-1}$ ), and show a dispersion behavior with characteristics rather well known from studies in simple polycrystalline fcc solids [26]. Also shown in Fig. 3 are the  $Q$  dependences of peak frequencies appearing at large wave vectors, and which can also be identified with pertinent features appearing in  $Z(E)$ , as well as the dispersion of higher-lying peak envelopes.

The wave-vector dependence of the reduced frequency moments is shown in Fig. 4, where the  $I(Q)$  inelastic intensity is depicted in the upper frame and the square roots of  $\omega_0^2$  and  $\omega_l^2$  are shown in the lower frame alongside with lines which mark the longitudinal and transverse sound velocities as measured by means of Brillouin light scattering [25]. As it can be clearly seen from the graph, both  $\omega_0$  and  $\omega_l$  show a steep increase in frequency up to  $Q = 0.9 \text{ \AA}^{-1}$ , where  $\omega_0$  reaches a maximum value of 8.6 THz, which closely corresponds to the frequency of the highest-lying peak in the translational manifold of the  $Z(E)$  shown in Fig. 1(a). The minimum at  $Q_p$  [i.e., around the position of the maxima of  $I(Q)$ ] corresponds to a frequency slightly above that of the first peak of the density of states (2 THz versus 1.6 THz), and the oscillations from such a minimum up to the largest explored wave vectors are confined within a frequency region of about 2–4 THz which basically corresponds to the extent of the acoustic peaks appearing in  $Z(E)$  [13, 14].

From what is shown in Figs. 3 and 4, it seems clear that the approach towards hydrodynamic sound occurs at fairly low wave vectors (below  $0.1 \text{ \AA}^{-1}$ ) which makes it extremely difficult to follow such a transition by means of INS or MD approaches.

The higher-lying modes are also compared with the spectral moments in Fig. 4(b). It can be seen from the figure that up to about  $Q = 0.6 \text{ \AA}^{-1}$ , the dispersion behavior of the most intense peak in  $J_l(Q, \omega)$  basically coincides with  $\omega_0$ . Again, from comparison with the straight lines which extrapolate the dispersion laws of hydrodynamic sound it is clear that, although within this region of wave vectors this ‘‘dispersion curve’’ can be interpreted as arising from the propagation of an excitation defined by a well-defined average frequency, no consequences regarding the deviation from the sound modes can be adduced since the whole of the translational band participates in such motions. From a comparison between the  $\omega_0$  spectral moment with the dispersion curves corresponding to the lowest-lying peaks as shown in Fig. 4(b), the following points become clear.

- A truly sound-mode manifold appears at low  $Q$  values in  $J_l(Q, \omega)$  but remains visible in the  $S(Q, \omega)$  all along the Brillouin zone, showing up to  $Q \approx 0.6 \text{ \AA}^{-1}$  a quasilinear behavior. At the lowest explored wave vectors such a dispersion curve joins the linear dispersion law corresponding to transverse sound.

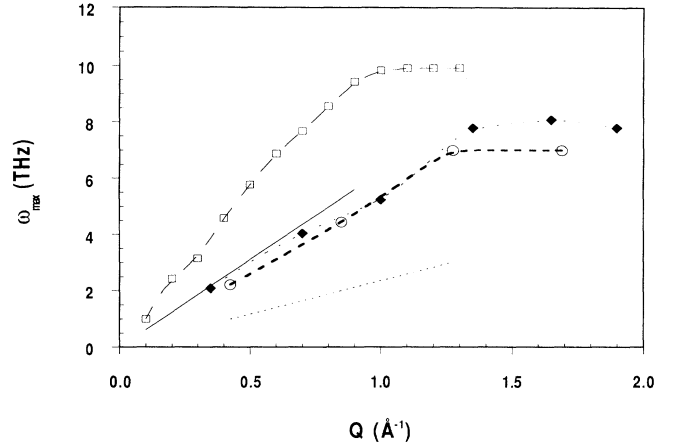


FIG. 5. A comparison of the  $\omega_{\max}$  characteristic frequencies of the main peak in the polycrystalline  $J_l(Q, \omega)$  (dashed line with squares) with that resulting from MD calculations of supercooled water [6] (dotted line with filled lozenges), or normal liquid [7] water (dashed line with open circles). The straight lines correspond to longitudinal sound for the polycrystal and normal liquid, respectively.

- Above  $Q_p/2$  the wave vector dependence of the above-mentioned excitation shows a nearly  $Q$ -independent behavior, and its characteristic frequency becomes rather close to that of  $\omega_0$ , and from its asymptotic value at high  $Q$  it may be assigned to mostly transverse sound waves, on the basis of its identification with a characteristic singularity appearing in the  $Z(E)$  density of states at such a frequency.
- A second peak becomes visible from about  $Q_p/2$  up to about  $2.2 \text{ \AA}^{-1}$ . It shows a vanishing frequency at  $Q_p$ , and its slope gives a sound velocity of about  $3800 \text{ ms}^{-1}$  which becomes close to that characteristic of longitudinal sound ( $3914 \text{ ms}^{-1}$  [25]). From such considerations it can be assigned to a mostly longitudinal sound wave which, due to the overlap with the other manifolds, only becomes well resolved within the second Brillouin zone.

A comparison between the results found in the present work with those previously reported for liquid water in its normal [7] or supercooled [6] states is finally made in Fig. 5. As can be easily seen from comparison of the curves corresponding to the polycrystal with those of the liquid, the steep, high-frequency curves which have been observed in the MD simulations are of a similar shape to the one of the polycrystal. It seems clear that if allowance is made for the strong softening of the elastic constants after melting, as evidenced by the linear dispersion depicting the hydrodynamic sounds, both curves corresponding to the polycrystal and liquid may be scaled to a common one [29].

#### IV. DISCUSSION AND CONCLUSIONS

Although the remarkable similarity between collective dynamical phenomena taking place in hot solids with

those of the same system upon melting at time and length scales accessible to INS or computer simulations has long been recognized, it has not been possible until very recently to quantitatively relate these excitations at both sides of the freezing transition. With the recent developments within the density-functional theory of freezing [30] it has become possible to establish a quantitative relationship between the phonon-dispersion curves in the crystal and quantities encompassing the liquid dynamics, at least for the simplest crystalline structures [31]. If such an endeavor still becomes impractical for complex fluids as the one we are dealing with, it is clear that conventional approaches based upon LD and MD computations as well as experiments can provide important insights into the intricate dynamics of these systems at microscopic scales.

Although a large number of calculations have been reported for either proton-ordered or -disordered ice polymorphs, the present communication constitutes an attempt to calculate the orientationally averaged dynamic structure factor on a realistic basis.

The collective dynamics of liquid water has been a controversial subject for a number of years, and it seemed difficult to reconcile the observations made with different theoretical or experimental tools. In comparison with other liquids studied up to the present moment [9, 32], the dynamical characteristics of this liquid even at microscopic scales manifest strong anomalies such as the ones described in the present paper, which has led to a number of speculative statements regarding the origin of the high frequencies appearing in computer simulation [6, 5] or in experimental contributions [8]. A remarkably similar behavior to the one found from the analysis of the polycrystalline dynamical structure factors was previously noticed for other associated liquid [9], where the wave vector dependence of the high values of the average excitation frequencies for wave vectors above  $0.6 \text{ \AA}^{-1}$  for both experimental and simulated spectra were found to

be originated from the strong buildup of an optical peak which dominates the spectral power from such  $Q$  values onwards. On the other hand, and contrary to the case of liquid water, the transition to the regime where the acoustic modes are well separated from the optical ones occurred in such a liquid at larger wave vectors ( $Q \approx 0.35 \text{ \AA}^{-1}$ ) which enabled INS and MD studies to follow this crossover in detail.

From the data and arguments exposed in the present paper, the physical origin of the steep "dispersion curves" has been clarified, and as a consequence, it seems clear that the dynamic response of such a liquid should be reexamined under a rather different light.

The results presented in this work are in agreement with the recent reinterpretation of the "fast-mode" frequencies in binary liquids, which are based on an analysis of the mode frequencies in terms of renormalized quantities due to damping effects, rather than the bare frequencies [33]. Once it is done, the dispersion curve for the fast mode appears as an opticlike excitation approaching a finite frequency at  $\lim Q \rightarrow 0$ , thus being characteristic of the motion of the light and heavy particles which exert out-of-phase oscillations [33].

The data reported herein also evidence the difficulty of approaching the problem from an experimental side, since rather large incident wave vectors would be required to cover a large dynamic range at small scattering angles, as required to follow the steep excitations up to  $Q \approx 0.9 \text{ \AA}^{-1}$ . With the advent of high-flux spallation neutron sources it should become possible in the near future to test the predictions made in the present work.

#### ACKNOWLEDGMENTS

This work has been supported in part by DGICYT Grant No. PB89-0037-C03, and EEC Contract No. SC1-CT91-0714(TSTS).

- 
- [1] A. Campa and E.G.D. Cohen, *Phys. Rev. Lett.* **61**, 853 (1988); P.B. Lerner and I.M. Sokolov, *Physica C* **150**, 465 (1988).
  - [2] J. Bosse, G. Jacucci, M. Ronchetti, and W. Schirmacher, *Phys. Rev. Lett.* **57**, 3277 (1986).
  - [3] G.H. Wegdam, A. Bot, R.P.C. Schram, and H.M. Schaink, *Phys. Rev. Lett.* **63**, 2697 (1990).
  - [4] W. Montfrooij, P. Westerhuis, V.O. de Haan, and I.M. de Schepper, *Phys. Rev. Lett.* **61**, 2155 (1988).
  - [5] R.W. Impey, P.A. Madden, and I.R. McDonald, *Mol. Phys.* **46**, 513 (1982); M. Wojcik and E. Clementi, *J. Chem. Phys.* **85**, 6085 (1986).
  - [6] S. Sastry, F. Sciortino, and H.E. Stanley, *J. Chem. Phys.* **95**, 7775 (1991).
  - [7] M.A. Ricci, D. Rocca, G. Ruocco, and R. Vallauri, *Phys. Rev. A* **40**, 7226 (1989).
  - [8] J. Teixeira, M.C. Bellisent-Funel, S.H. Chen, and B. Dorner, *Phys. Rev. Lett.* **54**, 2681 (1985).
  - [9] Experimental INS data regarding the liquid are given in F. J. Bermejo, F. Batallán, J. L. Martínez, M. García-Hernández, and E. Enciso, *J. Phys. Condens. Matter* **2**, 6659 (1990), and a comparison with MD and LD calculations in J. Alonso, F.J. Bermejo, M. García-Hernández, J.L. Martínez, W.S. Howells, and A. Criado, *J. Chem. Phys.* **96**, 7696 (1992).
  - [10] Experimental and simulation data regarding the glass phase are contained in F.J. Bermejo, D. Martín, J.L. Martínez, F. Batallán, M. García-Hernández, and F.J. Mompean, *Phys. Lett.* **A150**, 201 (1990); *Europhys. Lett.* **15**, 509 (1991); *Phys. Rev. B* **46**, 6173 (1992).
  - [11] Relevant diffraction work was first reported by S.W. Peterson and H.A. Levy, *Acta Crystallogr.* **10**, 70 (1957); G. Honjo and K. Shimaoka, *ibid.* **10**, 710 (1957). Some comprehensive reviews are available, in particular W.F. Khus and M.S. Lehmann, *Water. Sci. Rev.* **2**, (1986), and references therein.
  - [12] P. Faure and A. Kahane, *J. Phys. (Paris)* **28**, 944 (1967); P. Faure, *ibid.* **30**, 214 (1969).
  - [13] H.J. Prask, S.F. Trevino, J.D. Gault, and K.W. Logan, *J. Chem. Phys.* **56**, 3217 (1972).

- [14] J.C. Li, J.D. Londono, D.K. Ross, J.L. Finney, J. Tomkinson, and W.F. Sherman, *J. Chem. Phys.* **94**, 6770 (1991); D.D. Klug, E. Whalley, E.C. Svensson, J.H. Root, and V.F. Sears, *Phys. Rev. B* **44**, 841 (1991).
- [15] B. Renker, *Phys. Lett.* **A30**, 493 (1969).
- [16] A.J. Leadbetter, R.C. Ward, J.W. Clark, P.A. Tucker, T. Matsuo, and H. Suga, *J. Chem. Phys.* **82**, 424 (1985).
- [17] M. Marchi, J.S. Tse, and M.L. Klein, *J. Chem. Phys.* **85**, 2414 (1986).
- [18] R.E. Shawyer and P. Dean, *J. Phys. C* **5**, 1017 (1972); **5**, 1028 (1972).
- [19] G. Nielsen, R.M. Townsend, and S.A. Rice, *J. Chem. Phys.* **81**, 5288 (1984).
- [20] D.D. Klug, J.S. Tse, and E. Whalley, *J. Chem. Phys.* **95**, 7011 (1991).
- [21] W.L. Jorgensen, J. Chandrasekhara, J.D. Madura, R.W. Impey, and M.L. Klein, *J. Chem. Phys.* **79**, 926 (1983); H.J.C. Berendsen, J.P.M. Postma, and W.V. van Gunsteren, in *Intermolecular Forces*, edited by B. Pullman (Reidel, Dordrecht, 1981), p. 331.
- [22] A. Criado, A. Conde, and R. Marquez, *Acta Crystallogr. A* **40**, 696 (1984).
- [23] O. Haida, T. Matsuo, H. Suga, and S. Seki, *J. Chem. Thermodynamics* **6**, 815 (1974); P. Flubacher, A.J. Leadbetter, and J.A. Morrison, *J. Chem. Phys.* **33**, 1751 (1960).
- [24] W. Cochran, *Rep. Prog. Phys.* **26**, 1 (1963).
- [25] For the Raman spectra of the most common polymorphs see B. Minceva-Sukarova, W.F. Sherman, and G.R. Wilkinson, *J. Phys. C* **17**, 5833 (1984); P.T.T. Wong and E. Whalley, *J. Chem. Phys.* **65**, 829 (1976), and references therein concerning the infrared data. Data concerning light-scattering spectra can be found in V. Mazzacurati, C. Pona, G. Signorelli, G. Briganti, M.A. Ricci, E. Mazzega, M. Nardone, A. de Santis, and M. Sampoli, *Mol. Phys.* **44**, 1163 (1981). The data regarding the sound velocities and elastic constants have been taken from R.E. Gagnon, H. Kiefte, M.J. Clouter, and E. Whalley, *J. Chem. Phys.* **89**, 4522 (1988).
- [26] F. W. Wette and A. Rahman, *Phys. Rev.* **176**, 784 (1968).
- [27] For a recent application to the case of a Lennard-Jones chain see A. Cuccoli, V. Tognetti, A.A. Maradudin, and A.R. McGurn, *Phys. Rev. B* **46**, 8839 (1992).
- [28] Five principal elastic constants are needed to describe the mechanical properties of hexagonal ice. For a polycrystalline sample, the velocity of longitudinal and transverse sound waves is related to those propagating along the main symmetry directions in the single crystal through  $v_l = \int_0^{\pi/2} v_l(\phi) \sin(\phi) d\phi$ , where  $\phi$  stands for the angle between the crystal  $c$  axis and the wave vector of the sound waves. The transverse sound velocity is defined as  $v_t^2 = \frac{3}{4}(v_l^2 - \rho B)$ , where  $\rho$  stands for the density and  $B$  is the adiabatic bulk modulus. For a detailed account of optical Brillouin studies in both single-crystal and polycrystalline phases of ice, see Gagnon *et al.* [25] and J. Chem. Phys. **92**, 1909 (1990).
- [29] The ratio of the slopes of the straight (low- $Q$  region) portions of the apparent dispersion of the main peak to the hydrodynamic sound becomes 1.92 for the ice polycrystal 2.21 for normal water and 2.35 for supercooled water. The small difference in the ratios for the ice and water can be well accounted for if the mass difference between the heavy-water ice used for the LD calculations and light water used in the simulations is taken into consideration.
- [30] D. Oxtoby, in *Liquides, Freezing and the Glass Transition*, edited by J.P. Hansen *et al.* Les Houches, 1989, (North-Holland, Amsterdam, 1991), p. 147.
- [31] M. Ferconi and M.P. Tosi, *Europhys. Lett.* **14**, 797 (1991).
- [32] Collective excitations in liquid deuterium are reported in F.J. Bermejo, J.L. Martínez, D. Martín, F.J. Mompean, M. García-Hernández, and A. Chahid, *Phys. Lett.* **A158**, 253 (1991); for a molecular simple liquid see *J. Chem. Phys.* **96**, 8477 (1992), and for a dense dipolar fluid see *J. Chem. Phys.* **95**, 5287 (1991).
- [33] B. Fak and B. Dorner, Institut Laue Langevin Report No. 92FA008S, 1992 (unpublished).